# The zebrafish Znt1a$^{sa17}$ mutant reveals roles of zinc transporter-1a in embryonic development

Issa A Muraina[a,1], Nic R Bury[a,2], Annabella Scott[b], Anthony Graham[b] and Christer Hogstrand[a,*]

[a]King's College London, Department of Nutritional Sciences, School of Life Course Sciences, Metal Metabolism Group, London, UK
[b]King's College London, MRC Centre for Neuro-developmental Biology, London, UK
[1]National Veterinary Research Institute, PMB 01, Vom, Nigeria
[2]School of Science Technology and Engineering, University of Suffolk, Suffolk, UK

[*]Corresponding author

King's College London
Franklin-Wilkins Building 3.85
150 Stamford Street
SE1 9NH London
UK

Email of correspondence: christer.hogstrand@kcl.ac.uk
T. 0044 7848 4436
F. 0044 7848 4171



Issa A. Muraina; Nic R. Bury; Annabella Scott; Anthony Graham; Christer Hogstrand (2020). The zebrafish Znt1asa17 mutant reveals roles of zinc transporter-1a in embryonic development. Journal of Trace Elements in Medicine and Biology

The published source for the article is available here:
https://www.sciencedirect.com/science/article/abs/pii/S0946672X20300614

**ABSTRACT**

**Background**

Zinc is one of the vital micronutrients required through various developmental stages in animals. Zinc transporter-1 (ZnT1; Slc30a1) is essential in vertebrates for nutritional zinc uptake and cellular zinc extrusion. Knockout of ZnT1 is lethal in vertebrates and there are therefore few functional studies of this protein *in vivo*.

**Methods**

In the present study we characterised the embryonic development in a zebrafish Znt1a mutant (Znt1a$^{sa17}$) which is lacking the last 40 amino acids of Znt1a as generated by TILLING. In parallel experiments, we compared the development of a zebrafish embryo Znt1a morphant (Znt1a$^{MO}$) which was generated by knockdown of Znt1a using morpholino-modified oligonucliotides.

**Results**

The homozygous Znt1a$^{sa17}$ embryo is viable, but displays a subtle phenotype informing on the biological roles of Znt1a. The Znt1a$^{sa17}$ fish have delayed development, including attenuated epiboly. They further show a decrease in phosphorylated extracellular signal-regulated kinases 1 and 2 (pERK1/2), retarded yolk resorption, and impaired clearance of free $Zn^{2+}$ from the vitelline fluid and its storage in hatching gland cells. All these aberrations are milder versions of those observed upon knockdown of Znt1a by morpholinos. Interestingly, the phenotype could be rescued by addition of the cell-permeable zinc chelator, N,N,N',N'-tetrakis(2-pyridinylmethyl)-1,2-ethanediamine (TPEN) to the incubation medium and was

aggravated by addition of zinc(II). Thus, the Znt1a$^{sa17}$ mutant has a reduced ability to handle zinc and can be characterised as a hypomorph.

**Conclusion**

This study is the first to show that the last 40 amino acids of Znt1a are of importance for its role in zinc homeostasis and ability to activate the MAPK/ERK pathway contrary to what was previously thought.

**Abbreviations**

Zinc (Zn), Zinc transporter-1 (Znt1), Zinc transporter-1a (Znt1a), Solute linked carrier (Slc), Solute linked carrier 30a1 (Slc30a1), Extracellular signal-regulated kinases 1 and 2 (ERK1/2), morpholino-modified oligonucleotide (MO, morpholino), N,N,N',N'-tetrakis(2-pyridinylmethyl)-1,2-ethanediamine (TPEN), Mitogen-activated protein kinase (MAPK), Zinc or Iron regulated transport (Zrt or Irt)-like protein (Zip), Cation Diffusion Facilitator (CDF), C-Terminal cytosolic Domain (CTD), Targeting Induced Local Lesions in Genomes (TILLING), Tumor protein p53 (p53), Locked Nucleic Acid (LNA), Integrated DNA Technology (IDT), single nucleotide polymorphism (SNP), polymerase chain reaction (PCR), Digoxygenin (DIG), *In Situ* Hybridization (ISH), Inductively-Couple Plasma Mass Spectrometry(ICP-MS), Threonine (Thr), Tyrosine (Tyr), Znt1a wild-type zebrafish embryo (Znt1a$^{+/+}$), Znt1a homozygote mutant zebrafish embryo (Znt1a$^{sa17}$), Znt1a morpholino-injected zebrafish embryo/morphant (Znt1$^{MO}$), controlled/scrambled morpholino-injected zebrafish embryo (Control$^{MO}$).

**Key words:** Zebrafish, Slc30a1, ERK1/2, zinc, development

**INTRODUCTION**

In vertebrates, two families of proteins are responsible for movement of zinc across biological membranes, the 'Zinc Transporter' (ZnT/SLC30) family [1-2] and the 'Zinc or Iron regulated transport (Zrt or Irt)-like protein' (ZIP/SLC39) family [2-5]. Members of the ZnT family belong to the larger Cation Diffusion Facilitator (CDF) family, which occurs at all phylogenetic levels from bacteria and archaea to fungi, plants and animals [6]. ZnT1 was the first mammalian zinc transporter to be discovered and it is expressed throughout the body. Notably, it is required for movement of zinc across epithelia, such as intestine, kidney and placenta [7-9]. It localises to the plasma membrane and functions to transport excess cytoplasmic zinc out of the cells [7]. *ZnT1* (*Slc30a1*) was originally discovered as a gene coding for a transcript that conferred zinc resistance to an otherwise zinc-sensitive cell line [7]. The authors further found that zinc resistance was the result of a zinc efflux activity of ZnT1 protein. Homozygous deletion or knockout of the whole *ZnT1* gene in mice was shown to be embryonic lethal [10] whereas in *Caenorhabditis elegans* as well as in *Drosophila*, a loss-of-function mutation of their respective versions on the vertebrate ZnT1 resulted in viable animals, but with impaired growth and development [11-12].

Human ZnT1 appears to function as a $Zn^{2+}/H^{+}$ exchanger [13], which is in accordance with the transporter mechanism operating in several prokaryotic CDF zinc exporters, including YiiP in *E. coli* [2, 14]. Like all known CDF proteins, ZnT1 has in addition to its transmembrane domains, a large C-Terminal cytosolic Domain (CTD), which are predicted to fold independently [2, 15-16]. In YiiP the CTD operates as a zinc sensor, allosterically triggering transport activity upon zinc binding by causing a structural rearrangement of the transmembrane domains, which enables zinc transport [14-15]. Such a function has not been demonstrated for eukaryotic family members, but functional complementation experiments have shown that the CTD is important for zinc transport function. Exogenous expression of rat ZnT1 conferred zinc resistance to an otherwise zinc sensitive hamster cell line, but a rat ZnT1 mutant lacking the CTD was unable to rescue the cells in culture medium with high zinc concentration [7]. A mutant lacking only the 72 last amino acids of the protein was reported to rescue the zinc sensitive phenotype, indicating that these may be dispensable for $Zn^{2+}$ transporter function.

In addition to being required as a zinc exporter, the CTD of both human ZnT1 and its *C. Elegans* counterpart, CDF-1, are positive regulators of the MAPK/ERK signalling pathway through direct protein-protein interaction with Raf-1 kinase and its regulator, 14-3-3 [17]. The CTD of ZnT1 is also a regulator of calcium homeostasis by controlling plasma membrane residency of both L- and T-type calcium channels [18-20].

The zebrafish (*Danio rerio*) is an important vertebrate model system, well suited for studies in genetics, embryology, development, and cell biology [21]. There is strong conservation between zebrafish and humans for most genes, which makes zebrafish an exellent model organism for studying complex biological processes [22]. Previous studies have demonstrated the utility of knockdown reverse genetics technologies in zebrafish to study the function of zinc importers, such as Zip6, Zip7 and Zip10 [23-25]. Although the function and regulation of Znt1 and other Znt proteins in fish have been characterised [26-28], we are aware of only a single published study on a zebrafish Znt mutant [29]. Zebrafish has two in-species paralogues of Znt1 (Znt1a and Znt1b; Ensembl Zv9). In the present study, we characterised a zebrafish mutant (sa17), which lacks the 40 last amino acids of the Znt1a protein and show that it has impaired embryonic development, zinc dysregulation, as well as disturbances in MAPK/ERK signalling. The mutant was a mild phenocopy of embryos subjected to Znt1a knockdown using morpholino modified oligonucleotides.

## MATERIALS AND METHODS

### Animal model

All experiments were performed in accordance with licences held under the UK Animals (Scientific Procedures) Act 1986 and later amendments and conforming to all relevant guidelines and regulations. Zebrafish embryos with a mutation in *slc30a1a* (*znt1a*; strain sa17) were generated through TILLING by the Sanger Centre [30] and outbred F2 mutants transferred to King's College London. This mutation caused a transition of nucleotide ''A'' to ''T'' at 1568 coding sequence (Fig. 1) leading to premature termination of the Znt1a protein sequences which resulted in a truncated protein, short of the last 40 amino acids. These embryos were reared to adults under standard fish husbandry practice and thereafter genotyped to recover the heterozygote carriers of the mutation. The mutants were further

outbred in several generations and embryos from different genotypes were collected and reared to adult for study of embryonic development of the homozygote mutant, which we refer to as Znt1a$^{sa17}$. Since the ZnT1a$^{sa17}$ mutant was generated by TILLING, they are in spite of the outbreeding likely to harbour mutations in other genes not screened. Therefore, Znt1a wild-type zebrafish (Znt1a$^{+/+}$) from crosses between heterozygote sa17 carriers were crossed and used as controls in experiments with homozygote Znt1a$^{sa17}$ embryos. Bioinformatic analysis of the gene mutation was carried out by Clustal Omega sequence alignment as well as by Eukaryotic Linear Motif tool (http://elm.eu.org/).

**Mutation detection and genotype classification**

A Locked Nucleic Acid (LNA) method was adapted for detection of single nucleotide polymorphism (SNP) mutation which was used to classify the genotype [31]. This is based on TaqMan assay which utilizes dual-labelled fluorescence probes (DLP) to discriminate between allele 'A' and 'T' in the target region of the genomic DNA of fish using a Real-Time PCR (qPCR) technique. The primers and probe sequence sets (Table 1) for the assay were designed and synthesized by Integrated DNA Technology (IDT). Since the LNA bases significantly increase the melting temperature ($T_m$$^oC$), the LNA dual-labelled probe (DLP) unlike standard DNA DLP are shorter and so offer an improved ability to distinguish mutations or SNP.

The method of genotyping was re-confirmed in a number of samples using conventional nested polymerase chain reaction (PCR) followed by sequence analysis of the target region. The primers for conventional PCR were designed by Sanger Centre's Zebrafish Mutation Project (Supplementary Table 1A &1B) and synthesized by Sigma. In this technique, both internal forward and reverse primers (P2 & P3) were further re-designed with M13 forward and reverse tail primers (lower case sequences) for bi-directional sequencing of the PCR products.

**Gene silencing**

Wild-type embryos of the Sanger strain and/or King's strain (KWT2) were micro-injected at 1-4 cell stage with 2-4ng of translational blocking anti-sense morpholino-modified oligonucleotides (MO) for *znt1a* gene knockdown (5'GCGGAGCACAGACAGAAACAAAAGCT3') (GENETOOLS, Philomath, USA) using a previously described protocol [32]. A scramble or mismatch MO (Random-control-MASO) was injected in a similar way to serve as injected

control along with un-injected wild-type control. Because of the possibility of off-target effects produced by most MOs as a result of *p53* gene activation causing a non-specific neuronal cell death [33-34], a *p53* translational blocking MO (5'GCGCCATTGCTTTGCAAGAATTG3') was co-injected with *znt1a* MOs in the ratio of 1.0 : 1.5 to suppress the *p53*-mediated apoptosis, and the result of the embryonic development was compared to that resulting from injecting *znt1a*$^{MO}$ alone. All embryos were incubated at 28.5$^{o}$C and monitored through developmental stages.

For exposure analysis, embryos were incubated in embryo water either supplemented with zinc by 100µM of $ZnSO_4$ or depleted of zinc by 5µM TPEN (N,N,N,N,-Tetrakis(2-pyridymethyl ethylene-diamine).

**Gene expression analysis**

Digoxygenin (DIG)-labelled anti-sense RNA probe for *znt1* gene was produced according to standard gene cloning procedure which was followed by *in vitro* transcription. The forward and reverse primer sequences used for amplification of the gene fragment gave a product size of 538bp (f: 5'AGACCCAGTCCACCAACAAG3'; r: 5'AGGACATGCAGGAAAACACC3'). This probe was used for gene expression analysis on 24 hpf embryos using the method of whole-mount *In Situ* Hybridization (ISH) as described by Thiese and Thiese, 2004 [35].

For quantitative real-time PCR (qPCR) of Znt1a transcripts in wild-type and homozygote mutant (Znt1a$^{+/+}$ and Znt1a$^{sa17}$), total RNA was isolated from 24 hpf of both embryos using TRIzol® (Invitrogen™) according to the manufacturer's protocol. Following first strand cDNA synthesis using the High Capacity Reverse Transcription kit (Applied Biosystems™), gene expression levels were analysed by real-time quantitative polymerase chain reaction (qPCR) on ABI Prism 7700HT Sequence Detection System using a hydrolysis probe assay. The probe and primer sets for genes of interest were designed using Roche Universal Probe Library software (www.universalprobelibrary.com) which gave a product size of 78bp (F: 5'gttaatgcggagcggaag3'; R: 5'atatggagcactgccattaatct3'; Probe; 5'cagcccgg3'). 18s rRNA was used as housekeeping gene as described before [28]. Cycle thresholds (Ct) were obtained for each of the test genes and for the housekeeping gene and the differences between these (ΔCt) was calculated. Quantitative measurement of gene expression was derived using the $2^{(-\Delta\Delta Ct)}$ method, also known as the Livak method (36-37). Data were expressed as ratios to the

control and normalised to the reference or housekeeping gene, 18s rRNA. Primer pairs for each gene were amplified with equal efficiency, as verified using serial dilutions of the respective cDNA.

**Total and free zinc analysis in embryo**

Chorionated (whole) embryos at 24 hpf of Znt1a homozygote mutants, Znt1a morphants and wild-types backgrounds were acid digested respectively and total zinc concentrations were measured using Inductively-Couple Plasma Mass Spectrometry (ICP-MS) (Perkin Elmer, ELAN 6100DRC) as previously described [28]. In a parallel experiment, free zinc ions ($Zn^{2+}$) were assayed in the embryos by both fluorescent spectrophotometer (Synergy$^{TM}$ HT) and epi-fluorescence microscope (Nikon eclipse 400) at 360/530nm excitation/emission wavelength using a synthetic ratiometric zinc-specific fluorophore termed ZTRS probe [38]. Presence of free $Zn^{2+}$ in zebrafish embryos was assessed by incubating 10µM of ZTRS probe solution with embryos at blastula and 24 hpf stages and then observed under epi-fluorescence microscope as described above or measured by fluorospectrophotometry on a plate reader (Synergy$^{TM}$ HT).

**Morphometry**

Wild-type, Znt1a$^{sa17}$ and ZnT1a$^{MO}$ embryos were collected at 24 hpf and the yolk size of five embryos from each group was measured using an inverted microscope with a ruler. Measurements were taken dorso-ventrally across the yolk sac and processed in image J.

**Phosphorylated-extracellular regulated kinase (ERK) 1/2 activity in embryos**

Using the immuno-staining technique, embryos at early to mid-gastrulation stages (5-8 hpf) were immuno-stained for phosphorylated extracellular regulated kinase 1 and 2 (pERK1/2) of the amino acid residues surrounding the phospho-Thr202 and Tyr204 of ERK/MAPK in Znt1a$^{sa17}$ homozygote mutants, Znt1a morphants and control wild-type as well as wild-type injected with a scrambled MO control. A primary antibody to pERK1/2 (Cell Signalling®; rabbit polyclonal, #4370S) was used at 1:100 dilution and a secondary antibody (Abcam®; goat anti-rabbit conjugated to Alexa Fluor 488, ab15007) was used at 1:200 dilution as previously described [39]. Expression of pERK1/2 proteins in stained embryos were observed under epi-fluorescence microscope. Expression of pERK1/2 (Cell Signalling®; rabbit polyclonal, #4370S,

1:2000 dilution) and total ERK1/2 (Cell Signalling®; rabbit polyclonal, #9102, 1:1000 dilution) was also analysed by western blotting technique on wild-type and mutant embryos as previously described [39].

## RESULTS

### Genetics and bioinformatics

A zebrafish Znt1a mutant, sa17 (Znt1$^{sa17}$), was generated by mutagenesis followed by exome sequencing of outbred progeny to identify mutations in Znt1a (*slc30a1a*) [30]. This line has an A>T point mutation in position 1568 of the coding sequence (Chromosome 20: position, 13894123-13913790 Ensembl Zv9), which introduces a premature stop codon resulting in truncation of the last 40 amino acids from the Znt1a protein (Fig 1A & B). Sequence analysis of this region using the Eukaryotic Linear Motif tool (http://elm.eu.org/) revealed several putative phosphorylation sites and a terminal PDZ Class 1 interaction motif (Fig 1C). The zebrafish *slc30a1a* gene is located on the positive strand of chromosome 20 between *nek2* and *rd3*. This block of genes is syntenic to Chromosome 1: 211649864-211848972 in human, which harbours the same genes in the same order, but on the negative strand. Znt1a protein is 59% identical to human ZNT1 and 67% identity to pufferfish (*Takifugu rubripes*) Znt1 (Fig 2), both of which have been demonstrated to be cellular zinc exporters [7, 13, 26]. Within the truncated C-terminal region of the Znt1a$^{sa17}$ mutant the highest degree of conservation is found at the 11 last amino acids including the PDZ motifs 'ESSL' contained in the C-termini of the fish and mammalian orthologs (Figs 1 & 2).

### *Slc30a1a* expression in wild-type, Znt1a$^{sa17}$, and Znt1a morphant embryos

*In situ* hybridisation for *Slc30a1a* showed that the transcript is predominantly expressed in the central nervous system, the yolk syncytial layer, and hatching glands of wild-type 24 hpf embryos (Fig. 3A). The Znt1a$^{sa17}$ mutant has a much less distinct *znt1a* mRNA transcript expression profile with a complete loss of detectable expression in the hatching gland cells and a more diffuse location of yolk syncytial layer cells (Fig. 3A). However, qPCR analysis of 24 hpf whole embryos revealed that there was no statistically significant overall difference in *znt1a*-mRNA levels in Znt1a$^{sa17}$ embryos, compared with the control (1.58±0.095-fold, Mean±SD, N=3). The efficacy of morpholino-mediated knockdown of *slc30a1a* was confirmed by the markedly reduced staining for *slc30a1a* mRNA in Znt1a morphant (Znt1a$^{MO}$) embryos.

**Znt1a mutation or knockdown causes delay in stages of embryo development**

The Znt1a$^{sa17}$ homozygote embryos were viable but showed slight morphological abnormalities in the form of delayed pigmentation and enlarged or unabsorbed yolk compared to wild-type embryos. These defects were also present in Znt1a morphant (Znt1a$^{MO}$) embryos (Fig 3B & C). Interestingly, the cell permeable zinc chelator, TPEN, alleviated the effects caused by the mutation/knockdown and zinc supplementation further slowed development (Fig 3B). In contrast, wild-type and control-MO embryos showed no change in response to either of these treatments (Fig 3B). A quantitative analysis of the size of the yolk for control wild type (Znt1a$^{+/+}$), control-MO (Control$^{MO}$), mutant (Znt1a$^{sa17}$), and morphant (Znt1a$^{MO}$) embryos at 24 hpf for different embryos revealed that it was significantly larger in both Znt1a$^{sa17}$ and Znt1a$^{MO}$ compared to the controls (Fig 3D). A behavioural defect of swimming in circles was also observed in morphant embryos as compared to controls.

***Znt1a* mutation or knockdown increases the free $Zn^{2+}$concentration in embryos**

There was no statistically significant difference in total zinc content between control wild-type (Znt1a$^{+/+}$), control-MO (Control$^{MO}$), mutant (Znt1a$^{sa17}$) and morphant (Znt1a$^{MO}$) embryos (Fig 4). The small molecule fluorescent zinc probe, ZTRS ($K_d$ = 5.7nM), was used to detect free $Zn^{2+}$ in embryos at 24 hpf. A significantly higher free $Zn^{2+}$ fluorescence signal was detected in Znt1a$^{sa17}$ and Znt1a$^{MO}$ whole embryos compared to the controls (Fig 4). This signal came from unabsorbed $Zn^{2+}$ present in the vitelline fluid in Znt1a$^{sa17}$ and Znt1a$^{MO}$ embryos as evidenced by weak ZTRS fluorescence in these embryos following dechorination (Fig 5A). The $Zn^{2+}$ signal from the chorion of the Znt1a$^{sa17}$ mutant was in contrast observed to be stronger than that from the wild-type control. Similarly, the hatching gland $Zn^{2+}$ fluorescence signal was reduced in Znt1a mutant (Znt1a$^{sa17}$) and Znt1a morphant (Znt1a$^{MO}$) embryos as compared to wild-type control in dechorionated embryo and this was further evidenced by addition of 100µM zinc, which totally obscured the hatching gland $Zn^{2+}$ signal in mutant and morphant embryos, but only partially in wild-type (5B). Experiment with embryos at epiboly stage also showed reduced $Zn^{2+}$ signal with ZTRS at the leading edge of the epiboly (white arrow) and blastoderm (red arrow) in mutant and morphant compared to wild-type and MO controls (5C). The $Zn^{2+}$ signal from the chorion of the Znt1a$^{sa17}$ mutant was in contrast stronger than that from the wild type control.

**Znt1a mutation or knockdown reduces activated ERK1/2 in embryos**

In 5 hpf wild-type embryos, there was clear staining of activated phosphorylated Znt1a ERK1/2 (pERK1/2) cells along the leading edge of the epiboly margin affecting the amino acid residues Thr202 and Tyr204 of ERK/MAPK kinase. In Znt1a$^{sa17}$ and Znt1a$^{MO}$ embryos, pERK1/2 staining was hardly visible indicating that pERK1/2 activity was reduced (Fig 6A). Expression of pERK1/2 was barely detectable by western blot in both mutant and wild-type, but total ERK1/2 was visible in both confirming the workability of the method (Fig 6B).

**DISCUSSION AND CONCLUSION**

Zinc is one of the vital micronutrients required through various developmental stages in zebrafish including the development of hatching gland [40] and expression of zinc metalloprotease hatching enzyme [41]. We have shown previously that pufferfish (*Takifugu rubripes*) Znt1 is a zinc efflux protein [26]. The results of the sequence alignment of ZnT1 from different vertebrate species shows that there is high degree of homology between zebrafish Znt1a and mammalian ZnT1 proteins including that from human (i.e. 96% similarity and 56% identity with human), indicating that this protein may perform a similar function in these species. The 40 C-terminal amino acids of Znt1a, which are missing in the Znt1a$^{sa17}$ mutant zebrafish, may also be important in the function of this protein because it contains an evolutionarily conserved terminal PDZ domain and possibly a binding site for 14-3-3 (CESKTPTLPSA) [42], which interacts with both human and *C. elegans* Znt1 orthologues [17]. In addition, the region contains predicted phosphorylation sites for GSK3 and CK1/2, both of which are key kinases in $Zn^{2+}$ signalling [25]. Most of these conserved motifs in zebrafish are also conserved in pufferfish Znt1 [26] supporting our experimental data showing that the 40-amino acid truncation of the C-terminus in zebrafish Znt1a is of importance for the function of the protein.

The more diffuse expression of the *znt1a* gene in the Znt1a$^{sa17}$ mutant and Znt1a$^{MO}$ embryos, especially around the yolk syncytial layer and the central nervous system, as observed in the present study by ISH, may point towards the role of Znt1a in neural function as well as zinc uptake from the yolk. This might explain behavioural aberrations (circling) and the reduced muscle mass observed in Znt1a morphant but with mild effect in Znt1a$^{sa17}$ mutant (Fig 3C). The reduced expression of Znt1a in the yolk syncytial layer might be indicative of impaired

zinc import, as futher evidenced by a higher level of $Zn^{2+}$ (measured by the fluorescent ZTRS $Zn^{2+}$ probe) in the vitelline fluid in both Znt1a$^{sa17}$ mutant and Znt1$^{MO}$ embryos with reduced $Zn^{2+}$ signal in the hatching gland and blastoderm (Fig 5A, B & C). The enlarged (unabsorbed) yolk in mutant and morphant embryos along with attenuated growth suggests that this also impaired absorption of other nutrients and not only zinc. Interestingly, loss of ability to absorb zinc has been shown to cause degeneration of the intestinal absorptive epithelium and also retard embryo development in rodent models [10, 43].

Although the free $Zn^{2+}$ concentration in the whole embryo (including vitelline fluid and chorion) was higher in the Znt1a$^{sa17}$ mutant and morphant, compared to the wild-type embryos, the total zinc concentration as measured by ICP-MS showed no statistically significant difference between the genotypes. The total zinc concentration in whole embryos agreed with previous studies where total zinc concentration per 24 hpf embryo was measured to be around 7.5ng [44-45]. Thus, only zinc distribution within the embryo is affected. This is not very surprising because the zinc present in the embryo is deposited in the egg by the female, who transfers zinc bound to the egg yolk protein, vitellogenin, from the liver to the developing oocyte and the homozygote Znt1a$^{sa17}$ embryos used in the present study were from the crossbred of two homozygote Znt1a$^{sa17}$ parents [46-47]. Total zinc measurement in embryo is unlikely to give complete information on zinc homeostasis, because the pool of 'free' $Zn^{2+}$, which is needed for the rapidly developing embryo and other biological processes, is very small compared to total zinc and can only be detected by fluorescent zinc sensors which can give more relevant information on zinc regulation [10]. Our finding of elevated free $Zn^{2+}$ signal intensity (using ZTRS probe) in the Znt1a$^{sa17}$ mutant and morphant embryos is supported by previous work in *Drosophila*, which used a genetically encoded protein zinc sensor (MtnB-EYFP) to show high free $Zn^{2+}$ signal intensity in an intestine-specific *Drosophila* Znt1 knockout [12].

Despite the effects of the Znt1a$^{sa17}$ mutation on growth and development, the homozygote mutant was viable as was the Znt1a morphant, but in contrast, ZnT1 knockout mice are embryonically lethal at 9$^{th}$ day of gestation [10]. This may be as a result of partial loss-of-function or altered function in the zebrafish mutation compared to the complete loss-of-function in the ZnT1 knockout mouse. It might also be as a result of the presence of another in-species paralogue of *znt1 (*i.e. *znt1b; slc30a1b*) in zebrafish which was also predicted to

contain the terminal PDZ domain as well as the same putative phosphorylation sites (GSK3 & CK2) as Znt1a, thus, potentially able to perform some compensatory function in absence or dysfunctional Znt1a paralogue. Mouse and other mammals, in contrast, have a single *Znt1* gene or transcript thus accounting for the lethal effect of gene disruption in these species.

As observed in the zebrafish Znt1a mutant and morphant, delayed development was also demonstrated in previous experiments in *C. elegans* with a loss-of-function mutation of the *cdf1* gene, which is considered to correspond to zebrafish *znt1a* [11]. This developmental delay may be connected to an impaired MAPK/ERK signalling in cdf1 mutant worms [11, 17, 19]. Cdf1 as well as human ZnT1 were shown to activate Raf1 through a physical interaction at the cytosolic C-terminal domain of either zinc transporter [11, 17, 19]. In agreement with these studies, Znt1a$^{sa17}$ mutant and morphant embryos showed reduced pERK1/2, indicating a suppression of the MAPK/ERK pathway. This could possibly be explained by loss of Raf-1 binding to Znt1a and suggests that the binding site might be located at the last 40 amino acids which are lacking in the Znt1a$^{sa17}$ mutant. It could potentially also be due to the inability of the Znt1a$^{sa17}$ mutants and Znt1a morphants to regulate intracellular free $Zn^{2+}$, which is a regulator of ERK1/2 through its role in inactivation of phosphatases [48]. The cells in the leading edge of the epiboly of wild-type embryos that stained for pERK1/2 also stained intensively for free $Zn^{2+}$ which may account for high $Zn^{2+}$ required for cellular proliferation at the blastoderm contrary to mutant and morphant with low zinc levels (Fig 5C). This could explain the increased activation of pERK in the wild-type due to $Zn^{2+}$ inhibition of protein phosphatases. The inhibition of ERK-directed phosphatase activity is observed whenever there is a concurrent increase in phosphorylated ERK1/2 [49]. The developmental defects and retardation observed in the zebrafish Znt1a$^{sa17}$ mutant and morphant are similar to the results of *erk2* morpholino-mediated knockdown in zebrafish embryos [39] and *Erk2* mutation in mouse embryos [50]. Knockdown of *erk2* in zebrafish also affects the cell migration processes during embryogenesis [39]. In the present study, there was a reduction in pERK1/2 with concomitant reduction in free $Zn^{2+}$ at the leading edges of the gastrula organiser cells in both Znt1$^{sa17}$ and Znt1a morphant embryos, providing a possible explanation for the delay of the epiboly. The high free $Zn^{2+}$ at the leading edge of the epiboly migration in wild-type embryos suggests that the increased ERK1/2 phosphorylation might be due to the effect of free $Zn^{2+}$ on phosphatase inhibition [48-49]. These observations lend further credence to support the

interaction between ZnT1 and MAPK pathway activation being necessary for diverse cellular process including cell growth, proliferation, differentiation, survival and vertebrate development [51]. The defect in signalling is thought to be responsible for hindering the epiboly migration thereby slowing down the development.

In conclusion, the Znt1a mutant ($Znt1a^{sa17}$) and morphant ($Znt1a^{MO}$) allowed us to study the functions of this zinc exporter *in vivo* and the results show that contrary to what was previously thought [7], the 40 C-terminal amino acids of the protein are important for its function(s). The deficiency of the mutant in zinc homeostasis was indicated through the efficacy of zinc and TPEN in manipulating the severity of the phenotype, and by the clear differences in free $Zn^{2+}$ distribution, as shown through *in vivo* $Zn^{2+}$ imaging. The mutant also revealed that the C-terminal fragment is involved in the ability of Znt1a to activate ERK1/2 which is due to interaction of Raf1 and 14-3-3 with its C-terminal domain [11, 17]. We further show with *in vivo* $Zn^{2+}$ imaging high levels of free $Zn^{2+}$ in the rapidly proliferating cells of the epiboly leading edge and how this is associated with Znt1a-dependent phosphorylation of ERK1/2.

A limitation of this study is that the $Znt1a^{sa17}$ mutant was generated by TILLING and is likely to have multiple mutations elsewhere in the genome. The chance that potential effects of mutations in other loci influenced the results in the present study were reduced by outbreeding and the use of wild type controls, which were offspring from wild type parents generated by crossing heterozygote sa17 carriers. The controls are therefore likely to include any other mutated genes, which allows us to conclude that the differences between $Znt1a^{sa17}$ and $Znt1a^{+/+}$ individuals were most probably caused by the *znt1a* mutation. In absence of wild-type Znt1a gene for phenotype rescue experiments, the parallel use of $Znt1a^{MO}$ embryos further helped to attribute the effects observed in the mutant to Znt1a deficiency.

**AUTHOR CONTRIBUTION**

IAM conducted all the experiments and drafted the manuscript; CH lead and supervised the project; NRB assisted in supervision of IAM; AS provided instruction in and supported zebrafish procedures; and AG provided support relating to evolutionary and development biology as well as laboratory techniques. IAM, CH, NRB, and AG contributed to editing of the manuscript.

**ACKNOWLEDGEMENTS**

Metal analysis was performed by Mr Andy Cakebread at the London Metallomics Facility funded by the Wellcome Trust (grant reference 202902/Z/16/Z). IAM was supported by a King's College London Graduate School Scholarship (KINGS) & Overseas Research Scholarship (ORS), and by a University of London Central Research Fund (CRF) grant. The ZTRS was a kind gift from Dr. Xu Zaochao from the D. Spring laboratory of Cambridge University. The authors wish to express their gratitude to the Executive Director NVRI, Vom for giving IAM the opportunity for further studies.

**CONFLICTS OF INTEREST**

The authors have no conflict of interest.

**REFERENCES**

1 R.D. Palmiter, L. Huang, Efflux and compartmentalization of zinc by members of the SLC30 family of solute carriers, Pflugers Arch. 447 (2004) 744-751.
2 C. Hogstrand, D. Fu, Zinc, in: W. Maret, A. Wedd, (Eds.), Binding, transport and storage of metal ions in biological cells. Roy Soc Chem, 2014, pp. 666-694.
3 B.H. Eng, M.L. Guerinot, D. Eide, M.H. Saie Jr., Sequence analyses and phylogenetic characterization of the ZIP family of metal ion transport proteins, J. Membr Biol. 166 (1998) 1-7.
4 M.L. Guerinot, The ZIP family of metal transporters, Biochim Biophys Acta. 1465 (2000) 190-198.
5 D.J. Eide, The SLC39 family of metal ion transporters, Pflugers Arc. 447 (2004) 796-800.
6 B. Montanini, D. Blaudez, S. Jeandroz, D. Sanders, M. Chalot, Phylogenetic and functional analysis of the cation diffusion facilitator (CDF) family: improved signature and prediction of substrate specificity. BMC Genomics. 8 (2007) 107.
7 R.D. Palmiter, S.D. Findley, Cloning and functional characterization of a mammalian zinc transporter that confers resistance to zinc, Embo J. 14 (1995) 639-649.
8 J.P. Liuzzi, R.J. Cousins, Mammalian zinc transporters, Annu Rev Nutr. 24 (2004) 151-172.
9 L.A. Lichten, R.J. Cousins, Mammalian zinc transporters: Nutritional and physiologic regulation. Annu Rev Nutr. 29 (2009) 153-176.
10 G.K. Andrews, H. Wang, S.K. Dey, R.D. Palmiter, Mouse zinc transporter 1 gene provides an essential function during early embryonic development. Genesis 40 (2004) 74-81.
11 J.J. Bruinsma, T. Jirakulaporn, A.J. Muslin, K. Kornfeld, Zinc ions and cation diffusion facilitator proteins regulate Ras-mediated signaling. Dev Cell. 2 (2002) 567-578.
12 X. Wang, Y. Wu, B. Zhou, Dietary zinc absorption is mediated by ZnT1 in Drosophila melanogaster, FASEB Journal 23 (2009) 2650-2661.

13 E. Shusterman, O. Beharier, L. Shiri, R. Zarivach, Y. Etzion , C.R. Campbell, I.H. Lee, K. Okabayashi , A. Dinudom , D.I. Cook, A. Katz A, A. Moran, ZnT-1 extrudes zinc from mammalian cells functioning as a Zn(2+)/H(+) exchanger, Metallomics 6:9 (2014) 1656-63.
14 S. Gupta, J. Chai, J. Cheng, R. D'Mello, M.R. Chance, D. Fu, Visualizing the kinetic power stroke that drives proton-coupled zinc(II) transport, Nature 7512 (2014) 101-4.
15 M. Lu, J. Chai, D. Fu D, Structural basis for autoregulation of the zinc transporter YiiP, Nat Struct Mol Biol. 16 (2009)1063-1067.
16 D.S. Parsons, C. Hogstrand, W. Maret, The C-terminal cytosolic domain of the human zinc transporter ZnT8 and its diabetes risk variant, FEBS Journal 285 (2018)1237-1250.
17 T. Jirakulaporn, A.J. Muslin, Cation diffusion facilitator proteins modulate Raf-1 activity, J Biol Chem. 279 (2004)27807-27815.
18 S. Levy, O. Beharier, Y. Etzion, M. Mor et al., Molecular basis for zinc transporter 1 action as an endogenous inhibitor of L-type calcium channels, J Biol Chem. 284 (2009)32434-32443.
19 O. Beharier, S. Dror, S. Levy, J. Kahn, M. Mor, S. Etzion, D. Gitler, A. Katz, A.J. Muslin, A. Moran, Y. Etzion, ZnT-1 protects HL-1 cells from simulated ischemia-reperfusion through activation of Ras-ERK signalling, J Mol Med (Berl). 30 (2011) 127-138.
20 M. Mor, O. Beharier, S. Levy, J. Kahn, S. Dror, D. Blumenthal, L.A. Gheber, A. Peretz, A. Katz, A. Moran, Y. Etzion, ZnT-1 Enhances the activity and surface expression of T-type calcium channels through activation of Ras-ERK signalling. Am J Physiol Cell Physiol. 303 (2012)192-203.
21 M. Westerfield, The Zebrafish Book: A Guide for the Laboratory Use of Zebrafish, The University of Oregon Press, Eugene, OR, 1993.
22 K. Howe, M.D. Clark, C.F. Torroja, J. Torrance, C. Berthelot et al., The zebrafish reference genome sequence and its relationship to the human genome. Nature 496 (2013) 498-503.
23 S. Yamashita, C. Miyagi, T. Fukada, N. Kagara, Y.S. Che, T. Hirano, Zinc transporter LIVI controls epithelial-mesenchymal transition in zebrafish gastrula organizer. Nature 429 (2004) 298-302.
24 G. Yan, Y. Zhang, J. Yu, Y. Yu, F. Zhang et al., 2012. Slc39a7/zip7 plays a critical role in development and zinc homeostasis in zebrafish. PLoS ONE 7(8), e42939.
25 K.M. Taylor, I.A. Muraina, D. Brethour, G. Schmitt-Ulms, T. Nimmanon, S. Ziliotto, P. Kille, C. Hogstrand, Zinc transporter ZIP10 forms a heteromer with ZIP6 which regulates embryonic development and cell migration, Biochem J. 15: 473 (2016) 2531-2544.
26 S. Balesaria, C. Hogstrand, Identification, cloning and characterization of a plasma membrane zinc efflux transporter, TrZnT-1, from fugu pufferfish (Takifugu rubripes), Biochem J. 394 (2006) 485-493.
27 G.P. Feeney, D. Zheng, P. Kille, C. Hogstrand, The phylogeny of teleost ZIP and ZnT zinc transporters and their tissue specific expression and response to zinc in zebrafish, Biochim Biophys Acta 1732 (2005) 88-95.
28 D. Zheng, G.P. Feeney, P. Kille, C. Hogstrand, Regulation of ZIP and ZnT zinc transporters in zebrafish gill: zinc repression of ZIP10 transcription by an intronic MRE cluster, Physiol Genomics 34 (2008) 205-14.
29 Z. Xia, J. We, Y. Li, J. Wang, W. Li, K. Wang, X. Hong, L. Zhao, C. Chen, J. Min, F. Wang, 2017. Zebrafish slc30a10 deficiency revealed a novel compensatory mechanism of Atp2c1 in maintaining manganese homeostasis. PLoS Genet. 13(7) e1006892.

30 R.N. Kettleborough, E.M. Busch-Nentwich, S.A. Harvey, C.M. Dooley, E. de Bruijn, F. van Eeden, I. Sealy, R.J. White, C. Herd, I.J. Nijman, F. Fényes, S. Mehroke, C. Scahill, R. Gibbons, N. Wali, S. Carruthers, A. Hall, J. Yen, E. Cuppen, D.L. Stemple, Systematic genome-wide analysis of zebrafish protein-coding gene function, Nature 496 (2013) 494-497.
31 M.P. Johnson, L.M. Haupt, L.R. Griffiths, 2004. Locked nucleic acids (LNA) single nucleotide polymorphism (SNP) genotype analysis and validation using real-time PCR. Nucl Acid Res 32(6), e55.
32 A. Nasevicius, & S.C. Ekker, Effective targeted gene "knockdown" in zebrafish, *Nat Genet.* 26 (2000) 216-220.
33 S.C. Ekker, J.D. Larson, Morphant technology in model developmental systems, Genesis 30 (2001) 89-93.
34 M.A. Pickart, E.W. Klee, A.L. Nielson, S. Sivasubbu, E.M. Mendenhall et al., 2006. Genome-wide reverse genetics framework to identify novel functions of the vertebrate secretome. PLoS One 1, e104.
35 B. Thiese, C. Thisse, Fast Release Clones: A High Throughput Expression Analysis. ZFIN Direct Data Submission 2004. http://zfin.org.
36 J.K. Livak, T.D. Schmittgen, Analysis of relative gene expression data using real-time quantitative PCR and the 2(-Delta Delta C(T)) Method. Methods 25 (2001) 402-408.
37 T.D. Schmittgen, K.J. Livak, Analyzing real-time PCR data by the comparative C (T) method. Nat Protoc 3(6) (2008) 1101-1108.
38 Z. Xu, K. Baek, H. Kim, J. Cui, X. Qian, D. Spring, I. Shin, J. Yoon, $Zn2^{+}$-triggered amide tautomerization produces a highly $Zn^{2+}$-selective, cell-permeable, and ratiometric fluorescent sensor, J Am Chem Soc. 132 (2010) 601-610.
39 S.F.G. Krens, S. He, G.E.M. Lamers, A.H. Meijer, J. Bakkers, T. Schmidt, H.P. Spaink, B.E. Snaar-Jagalska, Distinct functions for ERK1 and ERK2 in cell migration processes during zebrafish gastrulation, Dev Biol 319 (2008) 370-383.
40 D. Bourassa, S. Gleber, S. Vogt, C.H. Chong Hyun Shinc, J. Christoph, C.J. Fahrni, MicroXRF tomographic visualization of zinc and iron in the zebrafish embryo at the onset of the hatching period. Metallomics 8 (2016) 1122-1130.
41 V. Quesada, L.M. Sanchez, J. Alvarez, S. López-Otın, Identification and Characterization of Human and Mouse Ovastacin: A novel metalloproteinase similar to hatching enzymes from arthropods, birds, amphibians, and fish, J Biol Chem 279 (2004) 26627-26634.
42 F. Madeira, M. Tinti, G. Murugesan, E. Berrett, M. Stafford, R. Toth, C. Cole, C. MacKintosh, G.J. Barton, 14-3-3-Pred: improved methods to predict 14-3-3-binding phosphopeptides, Bioinformatics 31 (2015) 2276-2283.
43 J.P. Liuzzi, J.A. Bobo, L. Cui, R.J. McMahon, R.J. Cousins, Zinc transporters 1, 2 and 4 are differentially expressed and localized in rats during pregnancy and lactation. J Nutr. 133 (2003) 342-51.
44 R.T. Thomason, M.A. Pettiglio, C. Herrera, C. Kao, J.D. Gitlin, T.B. Bartnikas, 2017. Characterization of trace metal content in the developing zebrafish embryo. PLoS ONE 12(6): e0179318.
45 E. Ho, S. Dukovcic, B. Hobson, C.P. Wong, G. Miller, K. Hardin, M.G. Traber, R.L. Tanguay, Zinc transporter expression in zebrafish (Danio rerio) during development, Comp Biochem Physiol C Toxicol Pharmacol. 155 (2012) 26–32.
46 K.H. Falchuk, M. Montorzi, Zinc physiology and biochemistry in oocytes and embryos, Biometals 14 (2001) 385-395.

47 E.D. Thompson, G.D. Mayer, C.N. Glover, T. Capo, P.J. Walsh, C. Hogstrand, 2012. Zinc hyperaccumulation in squirrelfish (Holocentrus adscenscionis) and its role in embryo viability. PLoS One 7(10): e46127.
48 E. Bellomo, K.B. Singh, A. Massarotti, C. Hogstrand, W. Maret, The metal face of Protein Tyrosine Phosphatase 1B, Coord Chem Rev (2016) 327-328, 70-83.
49 D.J. Levinthal, D.B. DeFranco, Reversible oxidation of ERK-directed protein phosphatases drives oxidative toxicity in neurons, J Biol Chem 280 (2005) 5875–5883.
50 M.K. Saba-El-Leil, F.D.J. Vella, B. Vernay, L. Voisin, L. Chen, N. Labrecque, S.L. Ang, S. Meloche, An essential function of the mitogen-activated protein kinase Erk2 in mouse trophoblast development, Embo Rep. 4 (2003) 964-968.
51 B.A. Ballif, J. Blenis, Molecular mechanisms mediating mammalian mitogen activated protein kinase (MAPK) kinase (MEK)-MAPK cell survival signals, Cell Growth Diff. 12 (2001) 397-408.

**FIGURE CAPTIONS**

**Figure 1: Genetics and bioinformatics of the Znt1a$^{sa17}$ mutation**

(A) Schematic depiction of Znt1a protein showing the six putative trans-membrane (TM I-VI) domains. (B) Chemical mutagenesis of zebrafish caused A>T point mutation at position 1568 coding sequence (Chromosome 20: position, 13894123-13913790 Ensembl Genome Browser 95, Zv9) which introduced a premature stop codon causing truncation of the last 40 amino acids from the Znt1a protein. (C) Sequence analysis of the truncated region using the Eukaryotic Linear Motif tool (http://elm.eu.org/) revealed several putative phosphorylation sites and a terminal PDZ Class 1 interaction motif.

**Figure 2: Multiple sequence alignment of Znt1 from different species**

Clustal Omega multiple sequence alignment of ZnT1 gene for human (h), mouse (m), rat (r), zebrafish (z), Fugu (f) and Tetraodon (t) showing the six presumptive membrane-spanning domains (TMD I-VI) and conserved residues. Zebrafish has two Znt1 transcripts (a & b) with the 40 missing amino acids in Znt1a mutant shown in the aligned sequences of the C-termini highlighted by rectangular box containing the evolutionarily conserved PDZ class 1 interaction motif at the last 4 amino acids (i.e. ESSL) as well as other putative phosphorylation sites.

**Figure 3: Morphological phenotype caused by Znt1a C-terminal domain truncation or deficiency**

(A) Znt1a gene expression. Whole mount in situ hybridization (ISH) showing diffuse expression of znt1a mRNA in 24hpf *znt1a* homozygote mutant (Znt1a$^{sa17}$) and morphant (Znt1a$^{MO}$) embryos as compared to wild-type (Znt1a$^{+/+}$) and morpholino control (Control$^{MO}$) embryos, notably around the CNS & yolk syncytial layers (blue and red arrows) and also in the hatching gland (black arrow), which was completely absent in mutant and morphant embryos. (B) Untreated (Control) Znt1a$^{sa17}$ and Znt1a$^{MO}$ embryos show morphogenetic developmental delay at 33 hpf as compared to Znt1a$^{+/+}$ and Control$^{MO}$ embryos. Zn depletion by addition of 5 µM TPEN hastened the development of mutant and morphant embryos while 100 µM Zn supplementation further worsened their defects. Znt1a$^{+/+}$ and Control$^{MO}$ were not affected by the treatments. (C) Development of mutant Znt1a$^{sa17}$ and morphant Znt1$^{MO}$ at 24, 48, and 72hpf showing similar morphogenetic defects including retarded development, reduced pigmentation, and larger yolk sac as compared to Znt1a$^{+/+}$ and Control$^{MO}$ controls. At 72hpf the Znt1a$^{sa17}$ and the Znt1a$^{MO}$ embryos have unabsorbed yolk and the Znt1a$^{MO}$ has slender muscle mass, as shown by black and red arrows on the Znt1a$^{MO}$. (D) Yolk size diameter measurements in Znt1a$^{+/+}$, Znt1a$^{MO}$, and Znt1a$^{sa17}$ embryos using Image J. Data are presented as the mean ± SEM (n =5) where $p \leq 0.05$ is considered significant in a 1-way ANOVA, which was followed by Tukey's multiple comparison test. Groups that do not share the same letter are significantly different. All observational experiments (A-C) were conducted three times.

In each repeat, 100 Znt1a$^{+/+}$ and Znt1a$^{sa17}$ embryos and at least five Control$^{MO}$ and Znt1a$^{MO}$ were observed.

**Figure 4: Total zinc content and free $Zn^{2+}$ concentrations in whole embryos**

Total zinc was analysed by ICP-MS and relative free $Zn^{2+}$ concentrations estimated by capturing the signal from the ZTRS $Zn^{2+}$probe by fluorospectrometry at 24hpf in wild-type (Znt1a$^{+/+}$), *znt1a* sa17 mutant (Znt1a$^{sa17}$), *znt1a* morphant, (Znt1a$^{MO}$), and morpholino control (Control$^{MO}$) embryos. Data are presented as the mean ± SEM (n =5). Groups that do not share the same letter are significantly different at $p \leq 0.001$ in a 1-way ANOVA followed by Tukey's multiple comparison test.

**Figure 5: Truncation of the C-terminal domain of Znt1a or Znt1a knockdown causes redistribution of free $Zn^{2+}$ within embryos**

(A) Fluorescence microscope analysis showing increased ZTRS $Zn^{2+}$ fluorescence in the chorion/perivitelline fluid of homozygote *znt1a* sa17 mutant (Znt1a$^{sa17}$) and *znt1a* morphant (Znt1a$^{MO}$) embryos compared to wild-type control (Znt1a$^{+/+}$) and morpholino control (Control$^{MO}$). Note the absence of $Zn^{2+}$ fluorescence in the chorion of wild-type embryo and presence of fluorescence in the chorion of mutant embryo following embryo dechorionation. (B) Exposure of whole (chorionated) embryos to 100µM zinc and analysis of their free $Zn^{2+}$ fluorescence intensity in the hatching gland cells (HGC) after dechorionation at 24hpf showed reduced $Zn^{2+}$ fluorescence in Znt1$^{+/+}$ but total lack of fluorescence in Znt1a$^{sa17}$ and Znt1a$^{MO}$ embryos. HGC fluorescence is only blocked completely in Znt1a$^{+/+}$ by 200µM Zn. (C) The concentration of free $Zn^{2+}$ (ZTRS fluorescence) is high in the blastula (red arrows) with highest concentration occurring along the leading edge (white arrow) in Znt1a$^{+/+}$ and Control$^{MO}$ controls. In contrast the free $Zn^{2+}$ fluorescence is barely visible in Znt1a$^{sa17}$ mutant and Znt1$^{MO}$ morphant embryos.

**Figure 6: Truncation of the C-terminal domain of Znt1a or Znt1a knockdown causes loss of phospho-ERK during epiboly**

(A) Immunohistochemistry technique revealed stronger staining of phospho-ERK 1/2 and more advanced migration of phospho-ERK 1/2 positive cells at the leading edge at 5hpf (50% epiboly) in wild-type (Znt1$^{+/+}$) and morpholino control (Control$^{MO}$) embryos compared to *znt1a* sa17 mutant (Znt1$^{sa17}$) and *znt1a* morphant (Znt1$^{MO}$) embryos. (B) There was no difference in expression of total ERK1/2 protein as measured by Western blot between whole wild-type and *znt1a* sa17 mutant embryos at 24hpf. pERK was barely detectible in whole embryos of either genotype.

# Figure 1
# Figure 2



*Z Class 1*

# Figure 3

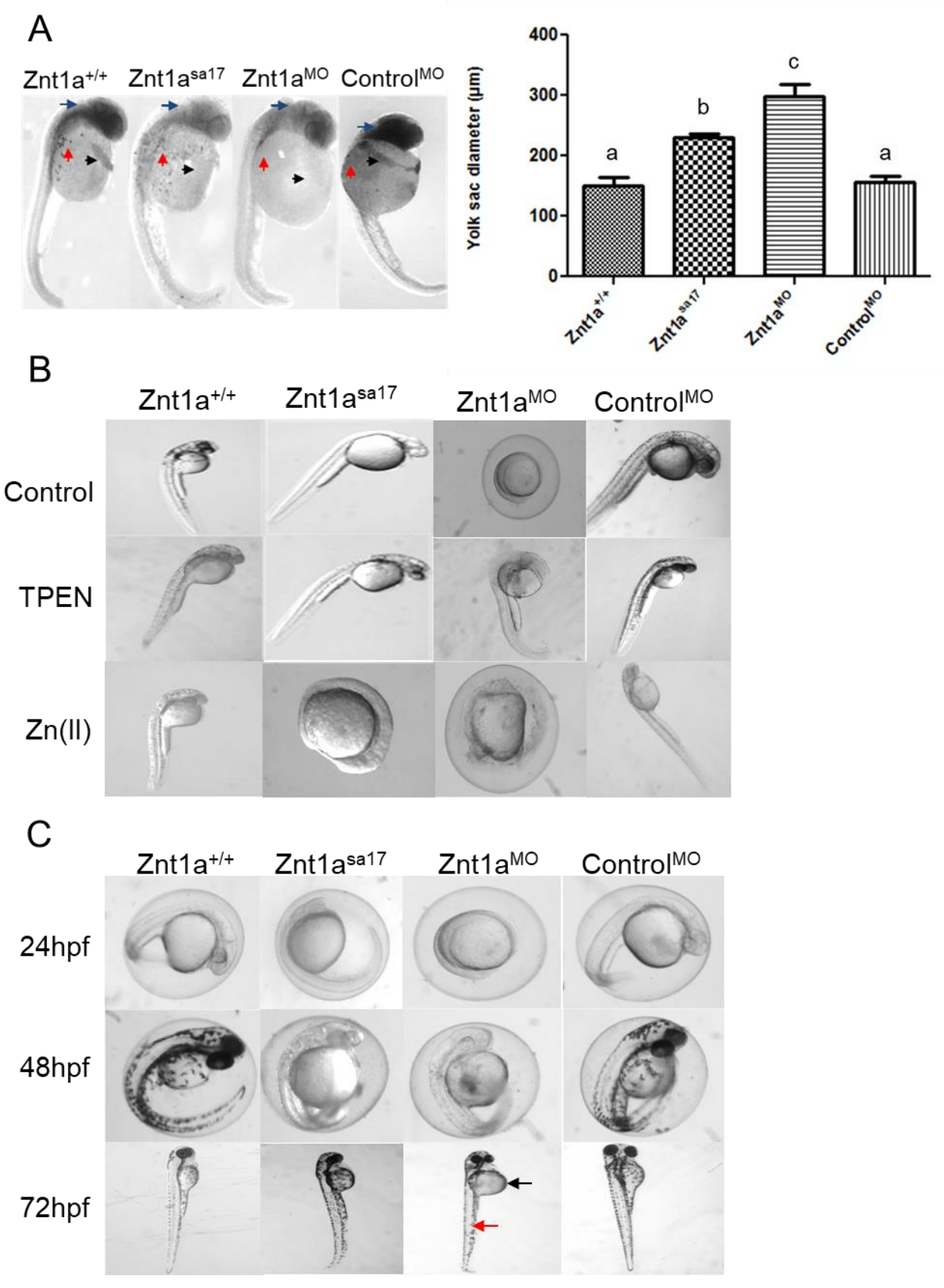
A
Znt1a+/+
Znt1asa17
Znt1aMO
ControlMO
Yolk sac diameter (μm)
400
300
200
100
0
a
b
c
a
Znt1a+/+
Znt1asa17
Znt1aMO
ControlMO
B
Znt1a+/+
Znt1asa17
Znt1aMO
ControlMO
Control
TPEN
Zn(II)
C
Znt1a+/+
Znt1asa17
Znt1aMO
ControlMO
24hpf
48hpf
72hpf

# Figure 4

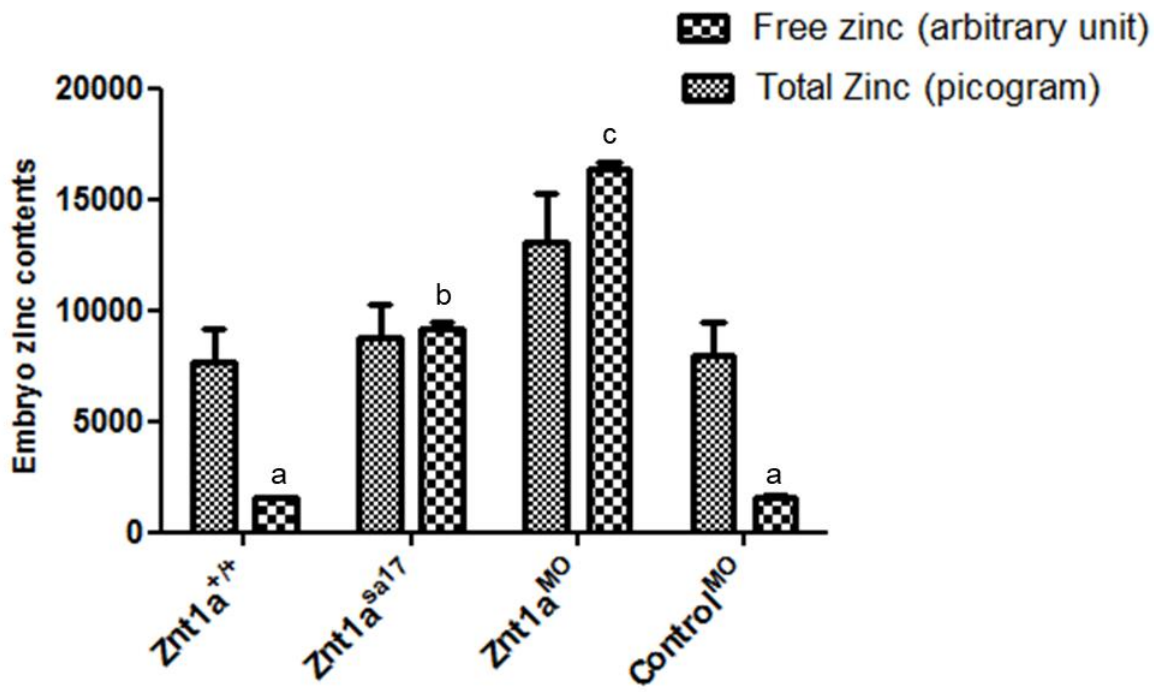
Free zinc (arbitrary unit)
Total Zinc (picogram)
Embryo zinc contents
20000
15000
10000
5000
0
a
b
c
a
Znt1a+/+
Znt1asa17
Znt1aMO
ControlMO

# Figure 5

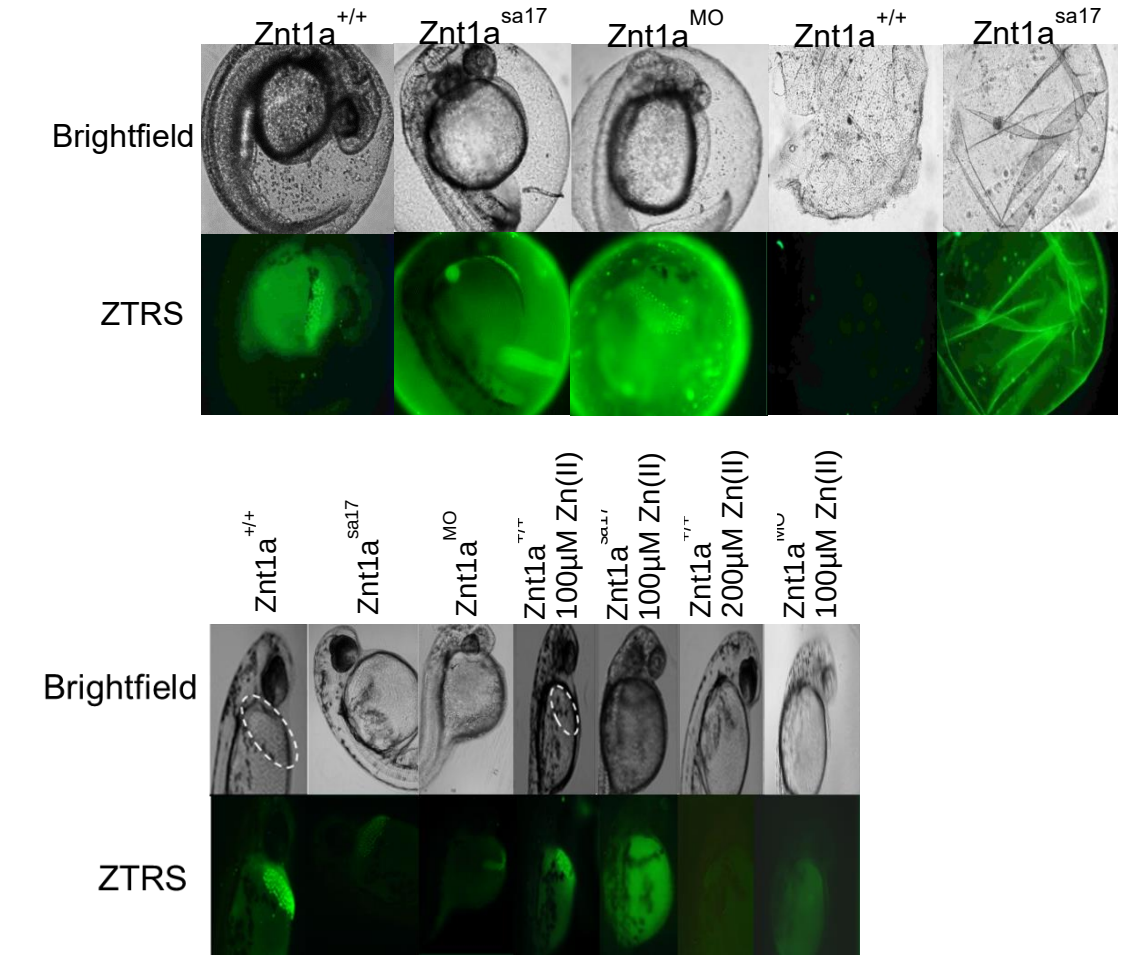
Znt1a+/+
Znt1asa17
Znt1aMO
Znt1a+/+
Znt1asa17
Brightfield
ZTRS
Znt1a+/+
Znt1asa17
Znt1aMO
Znt1a+/+ 100µM Zn(II)
Znt1asa17 100µM Zn(II)
Znt1a+/+ 200µM Zn(II)
Znt1aMO 100µM Zn(II)
Brightfield
ZTRS
Znt1a+/+
Znt1asa17
Znt1aMO
ControlMO
Brightfield
ZTRS

# Figure 6

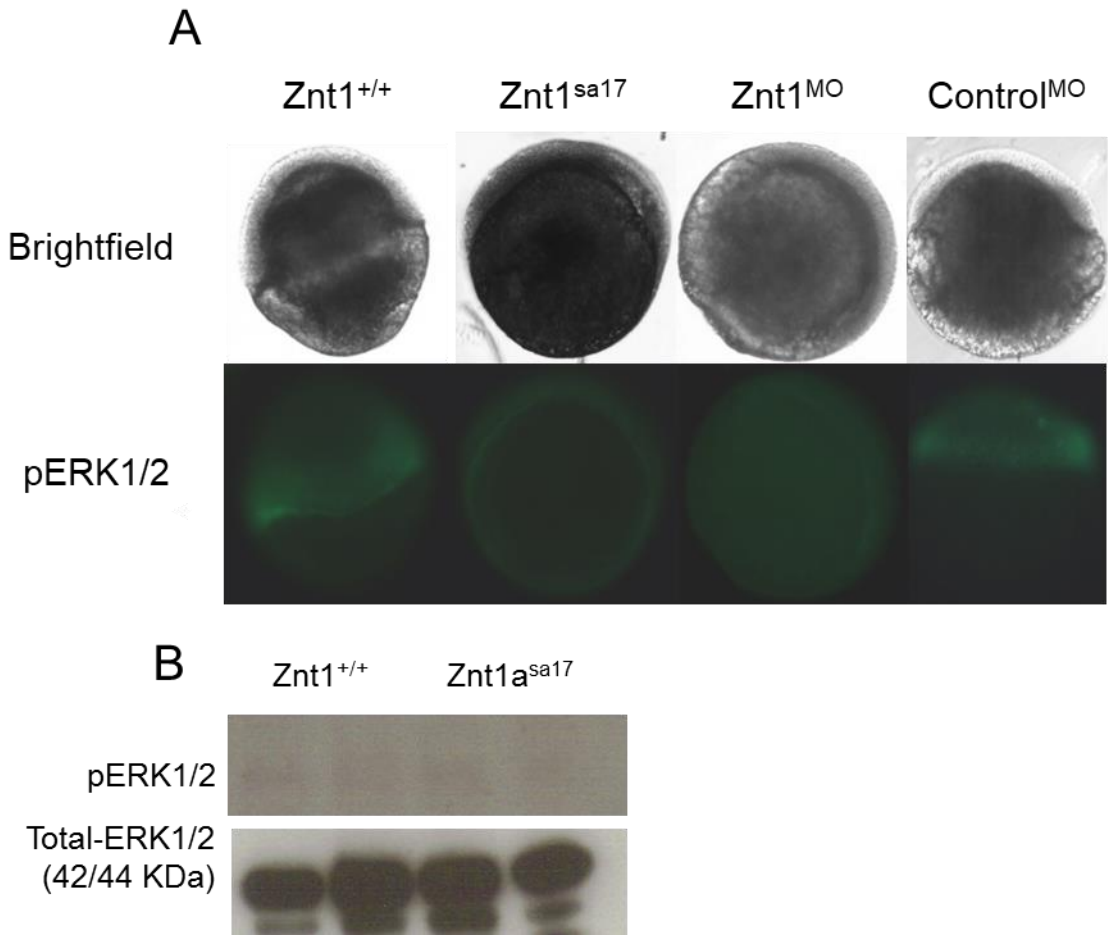
A
Znt1+/+
Znt1sa17
Znt1MO
ControlMO
Brightfield
pERK1/2
B
Znt1+/+
Znt1asa17
pERK1/2
Total-ERK1/2
(42/44 KDa)